WHITE PAPER

Verification of Dual-Scanning Lidar for Wind Resource Assessment

Examining the impact of recovery rate, range and synchronisation on reconstructed wind field data quality

Authors: Matthew Young, Andy Oldroyd, Maryam Shafa (Oldbaum Services); Anantha Padmanabhan Kidambi Sekar, Patrick Schwenk (Offshore Wind Consultants, OWC)

Based on: WESC 2023, 1.5 Mini Symposia — IEA Wind Task 52: Replacing Met Masts and Accelerating Offshore Wind Deployment (25 May 2023) https://doi.org/10.5281/zenodo.8034397

Oldbaum Services

Executive Summary

Dual-scanning lidar (DSL) is emerging as a viable alternative to fixed met masts for wind resource assessment (WRA) and site-condition assessment, both onshore and offshore. By combining two scanning lidars into a "virtual mast," DSL systems offer versatile measurement configurations able to acquire observations at distances beyond 10km , measure vertical wind shear and horizontal wind-field gradients, and resolve turbulence intensity (TI) close to conventional cup-anemometer equivalence. Despite this promise, industry uptake of DSL has been hindered by system complexity and price, unresolved questions about cup equivalence, and the absence of clear guidance.

To help address these issues, this paper summarises DSL performance from a verification campaign carried out at Janneby, Germany, using two Vaisala WindCube 400S pulsed lidars operating in dual-beam mode against an IEC-compliant 100 m met mast over a 68-day deployment (August–October 2022). The Janneby dataset — collected ahead of a lidar campaign deployment supporting site-condition assessment for the 2 GW West of Orkney offshore wind farm — was used to investigate three questions central to industry adoption of DSL:

- What is the baseline measurement performance of DSL, and how sensitive is it to sub-10-minute data availability(Recovery Rate; RR)?
- What is the impact of long measurement range on data quality?
- What is the impact of multi-height scanning and the associated loss of temporal alignment between heights on cup anemometer measurement equivalence?

The key finding is that DSL-derived wind speed and wind direction are highly accurate and closely cup-equivalent, remaining robust even at RR levels as low as 10%. Turbulence intensity is more sensitive to setup and sampling choices: it is systematically underestimated relative to cup measurements (attributable to the 100 m lidar probe length), it degrades with lower data-recovery rates, and it is the parameter most affected by both long sampling intervals in multi-height scans and timing misalignment between the two lidars. However, with careful consideration a 1%-difference to cup anemometers can be maintained.

Extending measurement range mainly reduces data availability rather than degrading accuracy directly. These results are intended to inform best-practice use of dual-scanning lidar deployment in offshore wind resource assessment.

This white paper presents the work shown at WESC Glasgow in 2023. The original presentation can be found on Zenodo: https://doi.org/10.5281/zenodo.8034397

Table of Contents

Table of Figures

1 Introduction and Motivation

1.1 Why Dual-Scanning Lidar?

Traditional wind resource assessment for offshore wind development has relied heavily on fixed meteorological (met) masts, which are large complex structures and expensive to install and maintain, especially at the water depths and distances from shore associated with modern offshore wind farm sites, e.g., hub heights in excess of 130m, and water depths in excess of 50m.

To address this, floating lidar systems (FLS) were introduced to the wind community, with adoption helped by the creation of The Carbon Trust Offshore Wind Accelerator roadmap for the commercial acceptance of floating lidar technology (The Carbon Trust 2018). While FLS is a great step forward to accessing wind measurements offshore, the technique is subject to some limitations when considering turbulence intensity (Gottschall, et al. 2014), and therefore a new solution was required for this key wind engineering parameter.

To address this, there has been some excellent studies on turbulence intensity measured by dual-scanning lidar (DSL; e.g. Shimada, et al. 2022; NEDO, 2023;; Watanabe, et al. 2021) which have shown that this measurement technique has great potential to provide cup-equivalent TI measurements for offshore applications.

DSL — in which two scanning lidar units are configured to intersect their beams at a common measurement point (Figure 1) — creates a series of "virtual masts" enabling wind observations to be obtained over a wide spatial area, as opposed to the single-grid-point location available to met masts or single virtual masts for FLS solutions.

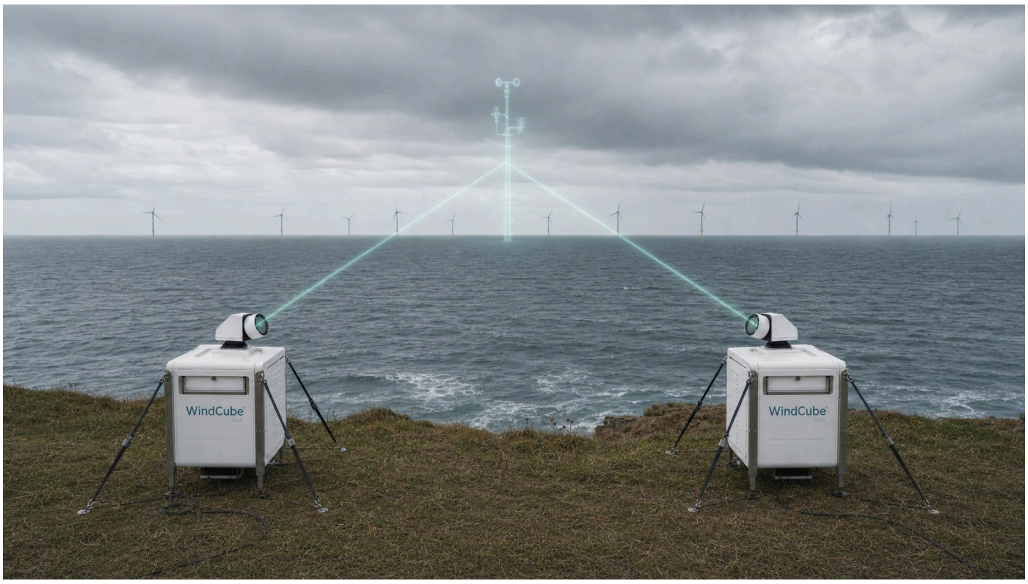

Figure 1: Sketch of a typical dual-scanning lidar setup when scanning offshore from onshore installation location to create offshore virtual met masts. Source: AI.

DSL offers several practical advantages over a single scanning lidar, an FLS or a physical met mast:

- **Acquisition at range**: measurements can be taken at distances of several kilometres from the lidar units, up to and potentially beyond 10 km, allowing flexible siting of the measurement equipment relative to the area of interest. In comparison to single scanning lidars, this is achieved with a DSL without increasing the measurement volume;
- **Multiple heights**: a single dual-lidar pair can sample several vertical levels sequentially, rather than requiring separate instrumentation at each height;
- **Horizontal gradients**: because the virtual mast location is not fixed to a physical structure, DSL configurations can in principle resolve horizontal gradients in the wind field.

A key advantage frequently cited in the literature is the potential for DSL to resolve turbulence intensity that is close to the "cup-equivalent" value obtained from a conventional cup anemometer (e.g., Peña & Mann, 2019; Shimada et al., 2022). However, several barriers have constrained industry uptake of this technology, including the operational complexity of dual-lidar systems and price, unresolved questions of cup equivalence for turbulence statistics, and — at the time of this study — the absence of accepted guidance for dual-scanning lidar deployment and data processing.

1.2 From Janneby to West of Orkney

The verification exercise described in this paper was carried out at the DNV test site in Janneby, Germany, prior to the deployment of the scanning lidar units for site-condition assessment in support of the West of Orkney Windfarm, a 2 GW offshore wind development off the coast of Orkney, Scotland.

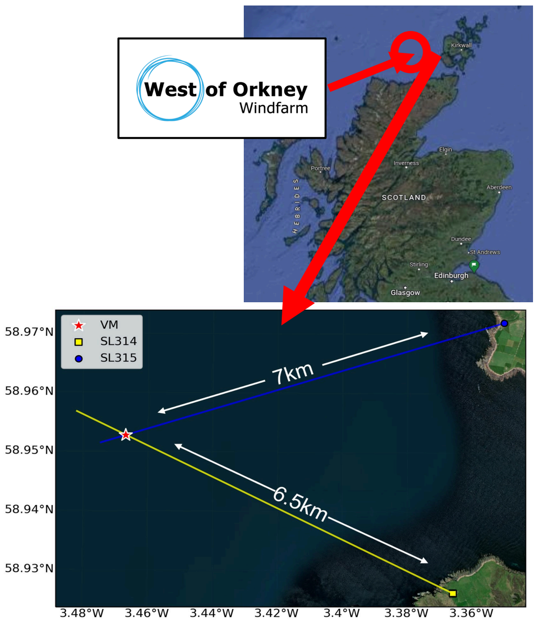

Figure 2: West of Orkney wind farm development dual-scanning lidar setup.

The Janneby dataset was used to examine three aspects of dual-lidar-mode capability and define data quality filtering over and above that recommended by Watanabe et al. (2021). This paper examines:

1. Measurement performance with respect to wind speed, wind direction and turbulence intensity, and its sensitivity to sub-10-minute data availability or recovery rate (RR);
2. Acquisition at long range, reflecting the greater distances anticipated in the offshore measurement campaign;
3. Temporal equivalence for multi-height scanning, reflecting the intended use of the dual-lidar system to sample multiple heights sequentially.

The lessons learned from this exercise directly informed the campaign data quality control and scan strategy options for the West of Orkney deployment.

Since this paper, IEA Wind Task 52 Working Group 6 has looked to independently verify the results observed in this paper in a datathon exercise.

2 Methodology

2.1 Test Site and Instrumentation

The verification test was conducted at Janneby, Germany, using two Vaisala WindCube 400S pulsed scanning lidars (units SL314 and SL315), each with a maximum range of >10 km. The two lidars were configured in a dual-beam arrangement with fixed dwell (stare mode) and intersecting beams, targeting a common measurement volume co-located with an IEC-compliant 100 m met mast (with two cup anemometers mounted at 103 m). The deployment ran for approximately 68 days, from August to October 2022.

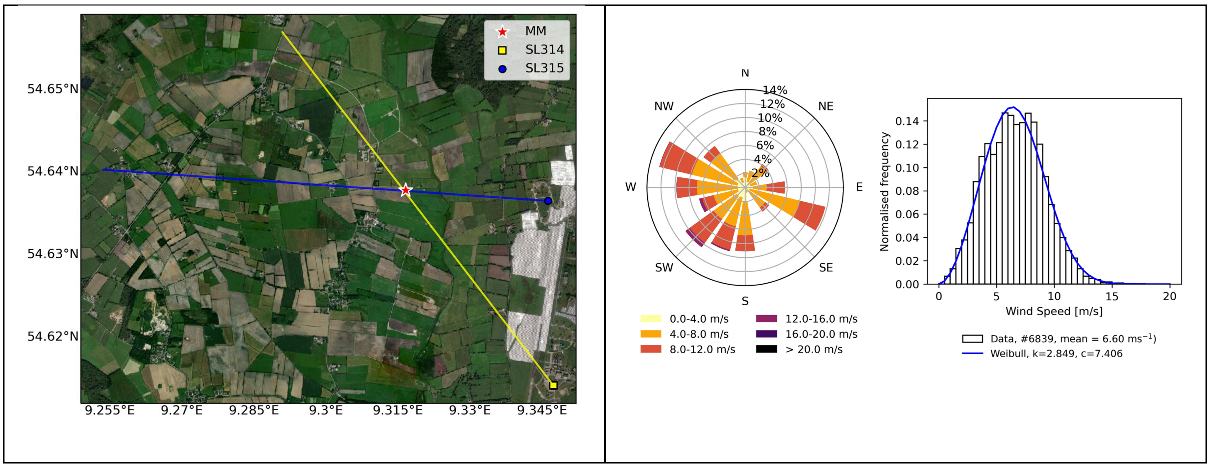

Figure 3: Janneby test setup showing the installation position of the two SL and the reconstruction point near the reference mast (left panel). Right panel shows the wind climate observed during the test period of about 68 days.

Key configuration parameters for the two lidar units are given in Table 1. The probe length (range gate length) of the lidars was set to 100m.

Parameter	SL314	SL315
Azimuth angle	322.85°	274.29°
Elevation angle	1.89°	2.72°
Range minimum	1000 m	1000 m
Range maximum	6000 m	6000 m
Range resolution	100 m	100 m

Parameter	SL314	SL315
Distance to met mast	3300 m	1900 m
Accumulation time	1 s	1 s

Table 1. Dual-lidar configuration parameters for the Janneby verification test.

The site exhibited a predominantly westerly/south-westerly wind rose, with a Weibull-fitted wind speed distribution (shape parameter k = 2.849, scale parameter c = 7.406 m/s) derived from 6,839 ten-minute observations with a mean wind speed of 6.60 m/s.

2.2 Horizontal Wind Reconstruction Approach

Each scanning lidar acquires wind data along the line-of-sight, returning a radial wind speed. For a 1s accumulation time, 1 Hz radial velocities from each lidar are initially quality-filtered based on:

- Carrier-to-noise ratio (CNR[1]), retaining values between −29 dB and −7 dB (Oldbaum internal valid range),
- Radial velocity outlier rejection, retaining values within the 10-minute mean ± 3 standard deviations (Watanabe, et al. 2021).

The combination of the LOS into the final wind data is shown schematically in Figure 4.

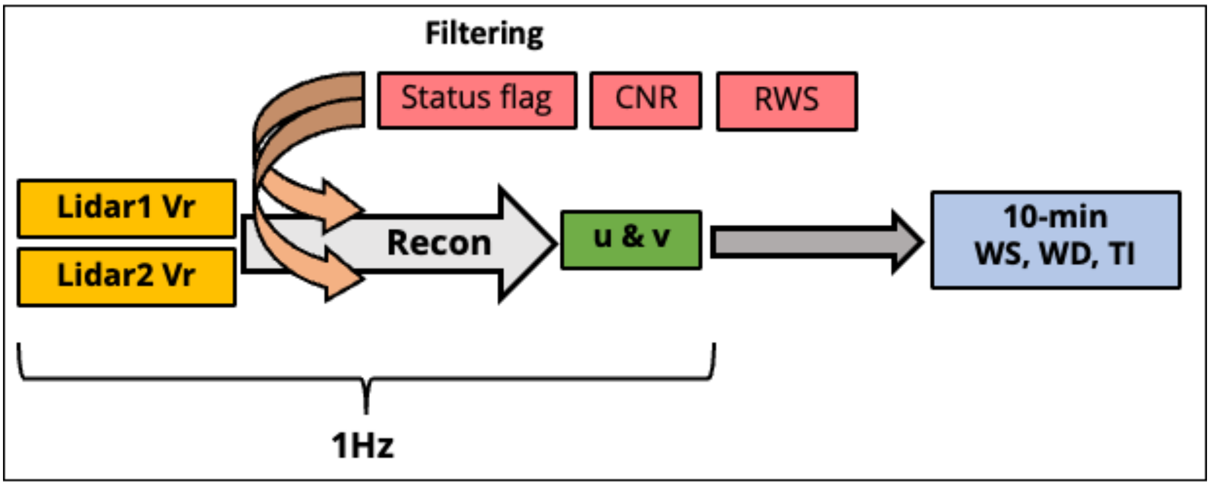

Figure 4: Schematic of the workflow showing the combination of LOS, the application of filters at the high-resolution level before the wind-field reconstruction takes place.

The radial velocity measured along a single lidar beam is related to the three-dimensional wind vector (u, v, w) by:

[1] CNR is a LOS quality filter particular to Vaisala. Other manufacturers should recommend their default quality filters according to their specific data processing approaches.

$$V_r = u\cos\theta\cos\phi + v\sin\theta\cos\phi + w\sin\phi$$

where θ is the lidar beam azimuth angle and ϕ is the beam elevation angle. Given the shallow elevation angles (<5°) used in this study, the vertical wind component (w) was assumed negligible, allowing the horizontal wind components (u, v) to be recovered directly from the two intersecting beams via:

$$u = \frac{u_{r1}cos\theta_2 \cos\phi_2 - u_{r2}cos\theta_1 \cos\phi_1}{\cos\phi_1 \cos\phi_2(\sin\theta_1 \cos\theta_2 - \sin\theta_2 \cos\theta_1)}$$

$$v = \frac{u_{r2}sin\theta_1 \cos\phi_1 - u_{r1}sin\theta_2 \cos\phi_2}{\cos\phi_1 \cos\phi_2(\sin\theta_1 \cos\theta_2 - \sin\theta_2 \cos\theta_1)}$$

where subscripts 1 and 2 denote the two lidar beams. The reconstructed u and v components were used to produce standard 10-minute mean wind speed (WS), wind direction (WD), and turbulence intensity (TI) statistics, following the processing workflow as shown in Figure 4: filtering (status flag, CNR, radial wind speed) → reconstruction (u, v) → 10-minute WS/WD/TI.

Verification is conducted by comparing the reconstructed wind field against the reference cup anemometer at the top height location. The cup is also subject to data cleaning where the data is filtered looking for mast shadow effects and site wake effects from nearby wind turbines or objects which may impact the quality of the comparison. Verification processes are governed by IEC standards such as IEC 50-2 for vertical profiling lidars (IEC 2022), with key performance indicators borrowed from The Carbon Trust roadmap (The Carbon Trust 2018).

2.3 Analysis of Range Sensitivity

To isolate the effect of measurement range independent of other factors, radial velocities recorded at the mast-intersection point were filtered concurrently using the same filtering criteria that would apply at longer ranges (up to the full 6000 m), allowing a like-for-like comparison of data availability and measurement accuracy as a function of range (Figure 5).

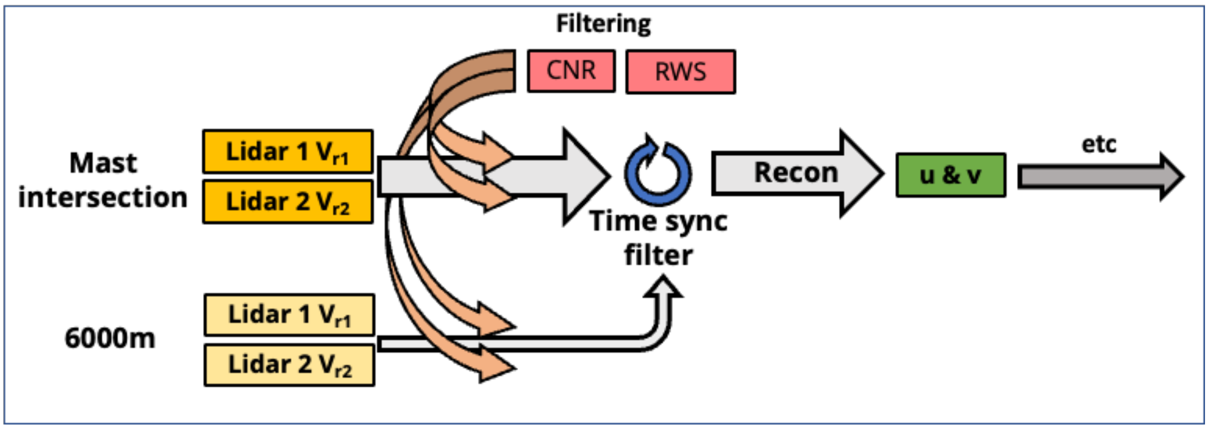

Figure 5: Data filtering process followed to imitate data loss at range (in this example 6000m), and its impact on data quality.

Please note whereas this process is able to capture the impact of data loss, it is not able to imitate the likely lower signal quality at further ranges and is therefore an incomplete comparison process. It should be noted that at the time of this presentation there were no long-range test sites available to the wind community. Since then, this shortfall has been addressed via the C-TEST[2] set up operated by Oldbaum Services in the UK, and by the Mutsu site in Japan, operated by MOC[3].

2.4 Analysis of Multi-Height Scanning and Temporal Equivalence

To evaluate the impact of multi-height scanning on measurement quality, a data-splitting method was applied to the 1 Hz dataset following the approach of Watanabe et al. (2021). The continuous 1 Hz dataset was subset into N discrete datasets, labelled as "heights", each with a specified sampling interval or dwell time, to emulate how a real multi-height scan would sample each height intermittently within a 10-minute period (Figure 6). Between each sequential dataset/height, 1 second of data was removed to represent data loss associated with physical scan-head movement between heights. Met mast data were left unmodified, serving as the temporally continuous reference. This method was applied across scenarios consisting of 3, 5, 6, 7 and 10 heights across a range of sampling intervals, to quantify how measurement statistics (R^2, bias, RMSE) for wind speed, wind direction, wind speed standard deviation, and TI change as the number of samples available at a point in space decreases.

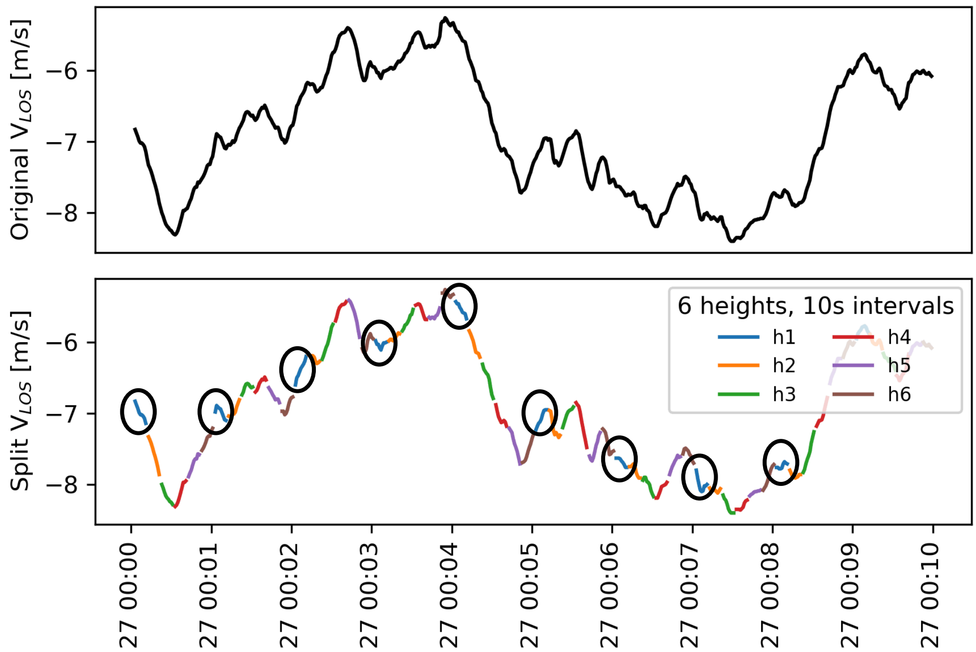

Figure 6: Schematic of the splitting method as defined in Watanabe, et al. (2021).

[2] For more information, contact : https://www.oldbaumservices.co.uk/lidar-testing
[3] For more information, contact: https://moc.or.jp/contact/

A similar approach was used to examine tolerance to temporal synchronisation error between the two lidars during multi-height scanning: a temporal lag (range: 0–60 s) was artificially applied to the 1 Hz measurements from the second lidar and the impact on correlation and error statistics reported.

3 Results

3.1 Baseline Performance and Sensitivity to Data Availability

Filtering the dual-lidar dataset by 10-minute data-recovery rate (the proportion of available 1 Hz samples within each 10-minute period) showed that wind speed and wind direction retained high accuracy ($R^2 > 0.99$) even at recovery rates as low as 10%, indicating that these parameters can be reliably estimated from comparatively sparse data (Figure 7). Turbulence intensity, by contrast, showed clear sensitivity to recovery rate: both R^2 and the regression slope for TI improved substantially as recovery rate increased, converging above roughly 50–60% recovery (Figure 7).

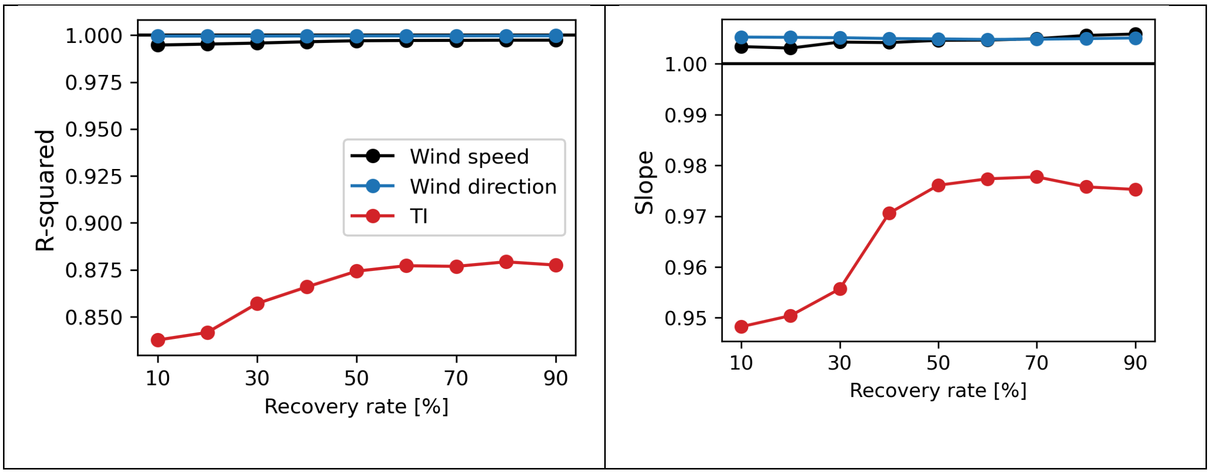

Figure 7: Impact of recovery rate on linear correlation for wind speed, wind direction and turbulence intensity

These results give clear guidance that separate filtering rules should be used when extracting quality wind speed and direction measurements versus turbulence intensity specific data.

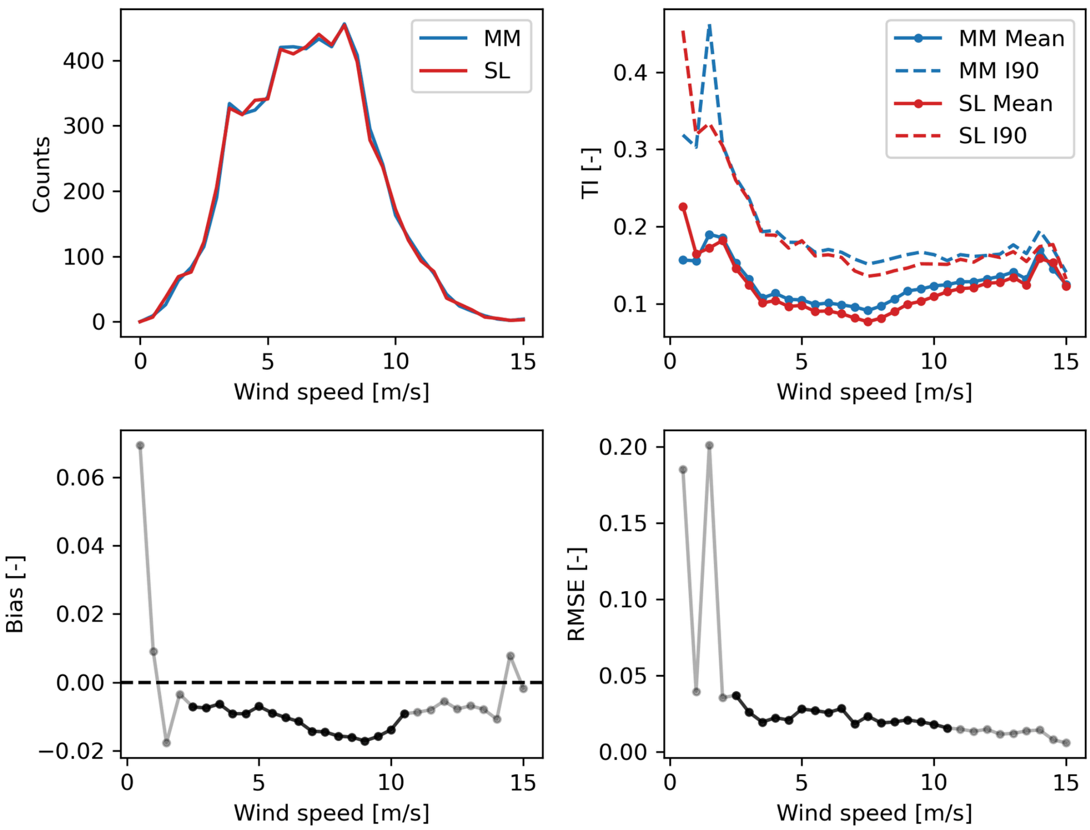

Figure 8: A more detailed look at TI comparison KPIs when using a Recovery Rate of 80%.

Figure 8 presents in more detail the quality of the TI dataset after applying a recovery rate filter of 80%. At an 80% recovery rate, mean TI and the representative TI metric I90 showed similar patterns between the dual-lidar system and the met mast cups, tracking closely across wind speed bins. However, a consistent underestimation of TI relative to the cups was observed, attributed to a constraint of the 100 m probe length (averaging volume) of the lidar beams relative to the point measurement of the cup anemometers.

3.2 Linear correlation comparisons

Direct line-of-sight comparisons between each lidar and the corresponding projected cup wind speed showed high agreement for the mean radial wind speed component (R^2 = 0.999 for both SL314 and SL315, slopes of 0.993 and 0.988, respectively), with good agreement for the line-of-sight wind speed standard deviation (R^2 of 0.921 and 0.936, slopes of 0.841 and 0.861), consistent with the greater sensitivity of turbulence-related statistics to measurement volume and averaging effects.

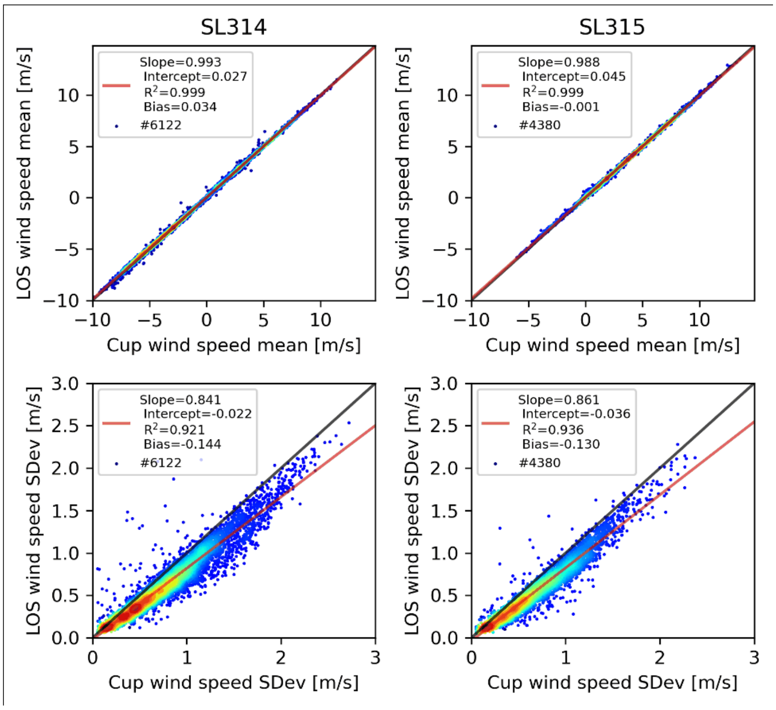

Figure 9: Line of sight comparisons for SL314 and SL315.

For the fully reconstructed horizontal wind, aggregated across the full dataset, dual-scanning lidar wind speed and direction showed near-unity slopes and R^2 values close to 1.000 relative to the met mast, while reconstructed TI showed a slope of 0.976 and R^2 of 0.879, again consistent with a modest underestimation bias.

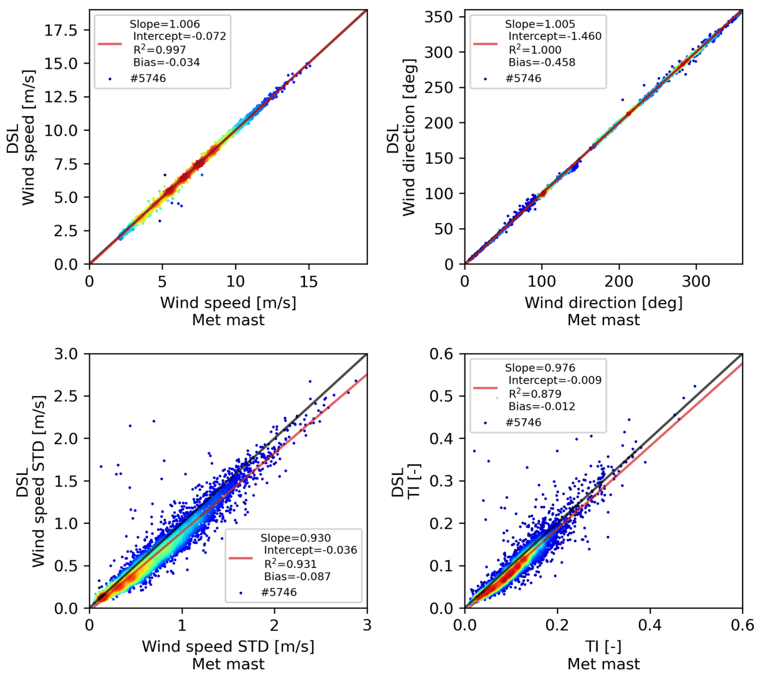

Figure 10: DSL wind field accuracy compared against a cup anemometer.

3.3 Impact of Measurement Range

Applying the data processing method outlined in Section 2.3, we see the impact of 10-minute data availability at different measurement ranges on the quality of wind speed and TI data from dual-scanning lidar in Figure 11. The additional impact of applying a 10% or 80%[4] recovery rate filter is also shown.

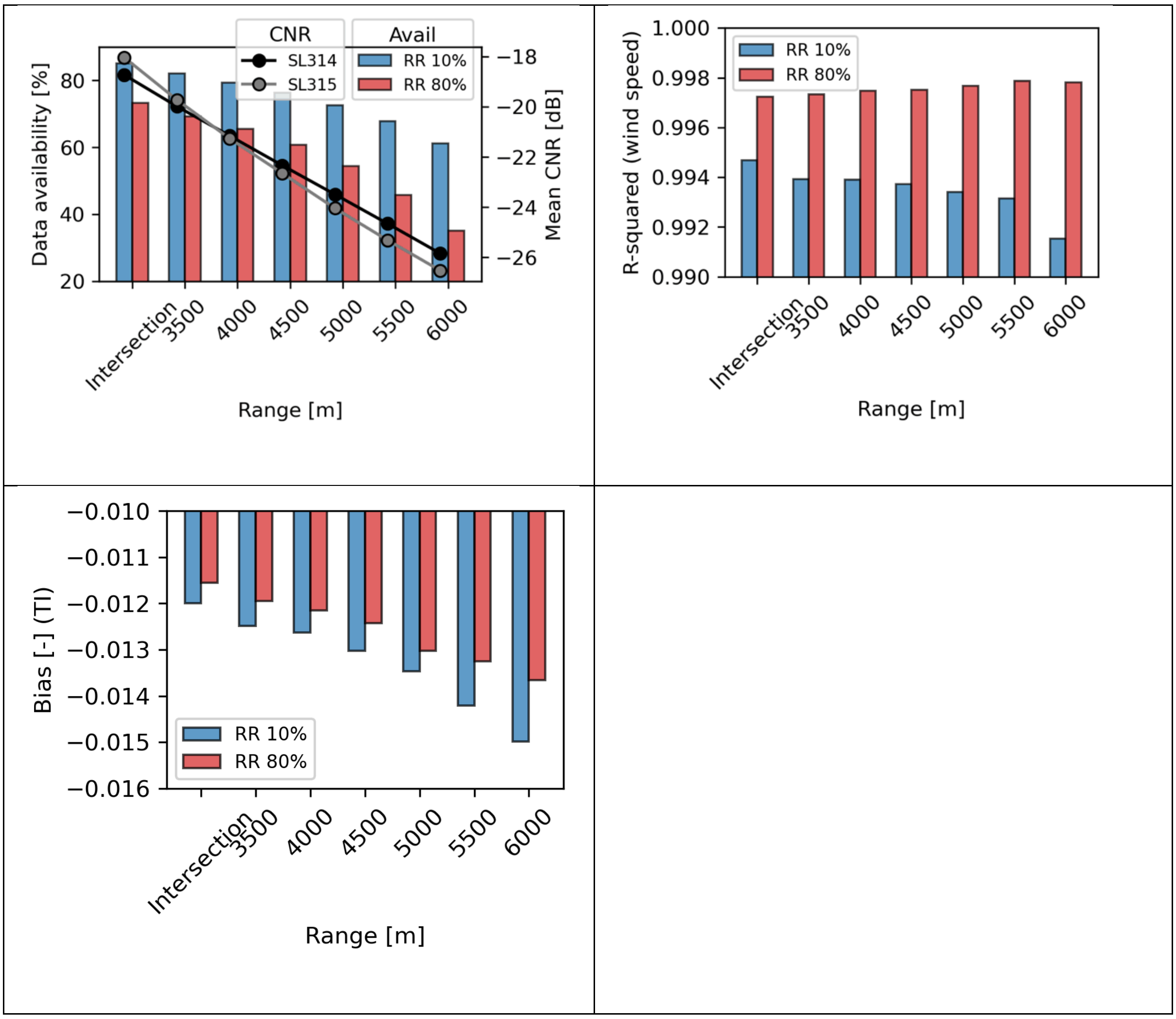

Figure 11: Impact of range on dual scanning lidar data quality

The approach presented in Section 2.3 is trying to imitate the impact of lower data availability at longer ranges, which is a common application of dual-scanning lidar. At Janneby, we can test at a range of 3 km, but campaign deployments are quite often used at ranges of 7 km or greater, so this impact has to be assessed.

Figure 11 shows that the dominant effect of increasing range is a reduction in data availability — from approximately 84% at the mast intersection down to approximately 64% at 6 km (Figure 11: top left

[4] Please note, as stated, the method applied here does not account for a reduction in CNR with range, and as such the application of the 80% filter at longer ranges may have a larger impact on data reduction than seen in this study.

panel) — driven by a corresponding decline in mean CNR with distance. The impact of range on measurement accuracy (R^2 for wind speed – Figure 9 top right panel, and TI bias – Figure 9 bottom left panel) was comparatively small. Wind speed R^2 is maintained at a level above 0.99 for both 10% and 80% recovery rates. The TI bias shows increasing negative bias with increasing range and increasing data loss. This can be seen for both 10% and 80% recovery rates, although it is possible to see that the impact on 10% recovery rate is progressively worse than the 80% case (i.e., the delta between 10% and 80% is increasing).

The analysis however only shows data quality for the remaining concurrent data from the DSL and the reference mast. As the number of samples decreases, the ability of the measurement to still acquire enough data to describe the wind climate it is trying to observe is called into question. This is not examined here, but the results shown in Figure 11 along with those from the IEA Wind Task 52 Datathon illustrate the need for a new KPI which is able to describe the representativeness of the observation after application of strict data quality filtering rules.

3.4 Impact of Multi-Height Scanning on Temporal Equivalence

To examine the impact of multi height scanning strategies on the data quality, the Watanabe et al., (2021) method is applied as per Section 2.4 and the resultant data population is shown in Figure 12 (right hand panel).

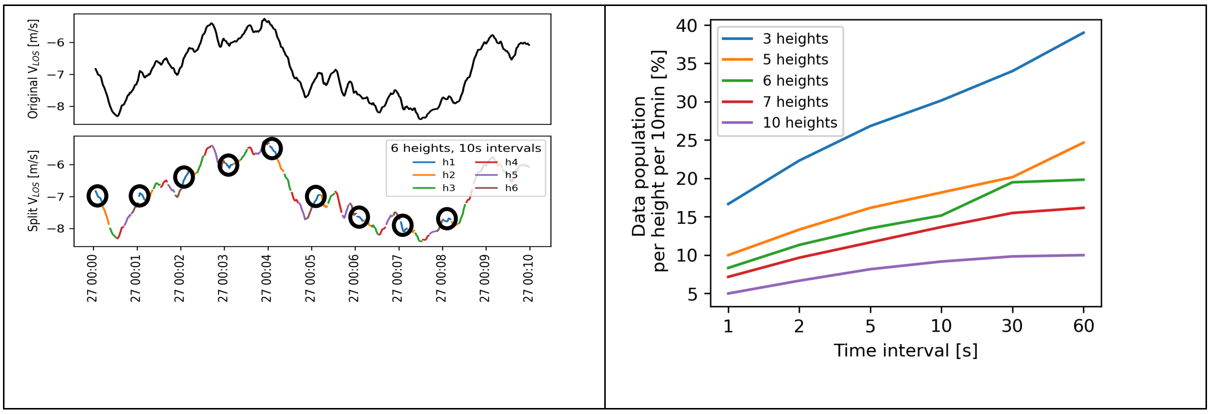

Figure 12: Extension of the Watanabe data splitting method to account for multi-height scan strategies

The multi-height scan strategy is simulated by splitting the continuous 1 Hz dataset into 3, 5, 6, 7 and 10 discrete heights, each with a specified dwell/sampling interval, plus a 1-second inter-height switch time. A similar approach was undertaken by Watanabe et al et al., (2021), but this study limited the dwell time to 10 seconds. The results presented here extends the analysis to account for shorter duration dwell times (down to 1 s) and also examines the impact of temporal synchronization by introducing an artificial time lag between the two scanning lidars.

Dwell time is defined as how long the scanning lidars focus on one point in space and acquire data. Therefore, a 10-second dwell timemeans the DSL focused for 10 seconds to acquire the wind speed data before moving onto the next point in the scan sequence. This is then repeated throughout a 10-minute scan sequence to produce the sub-10-minute dataset that then forms the reconstructed 10-

minute wind data. This has implications for recovery rate. Taking the example of an idealized 10-point scan sequence with 1 s dwell time and no lag, this setup would return a maximum of only 60 datapoints per 10-minute sequence. Applying a 10% recovery rate on this value would suggest that only 6 points are required to accurately describe the 10-minute dataset. Oldbaum do not believe this to be the case and that the lower end recovery rate should always be chosen when considering the scan strategy and that a minimum number of data points per 10-minute should be applied as lower limit.

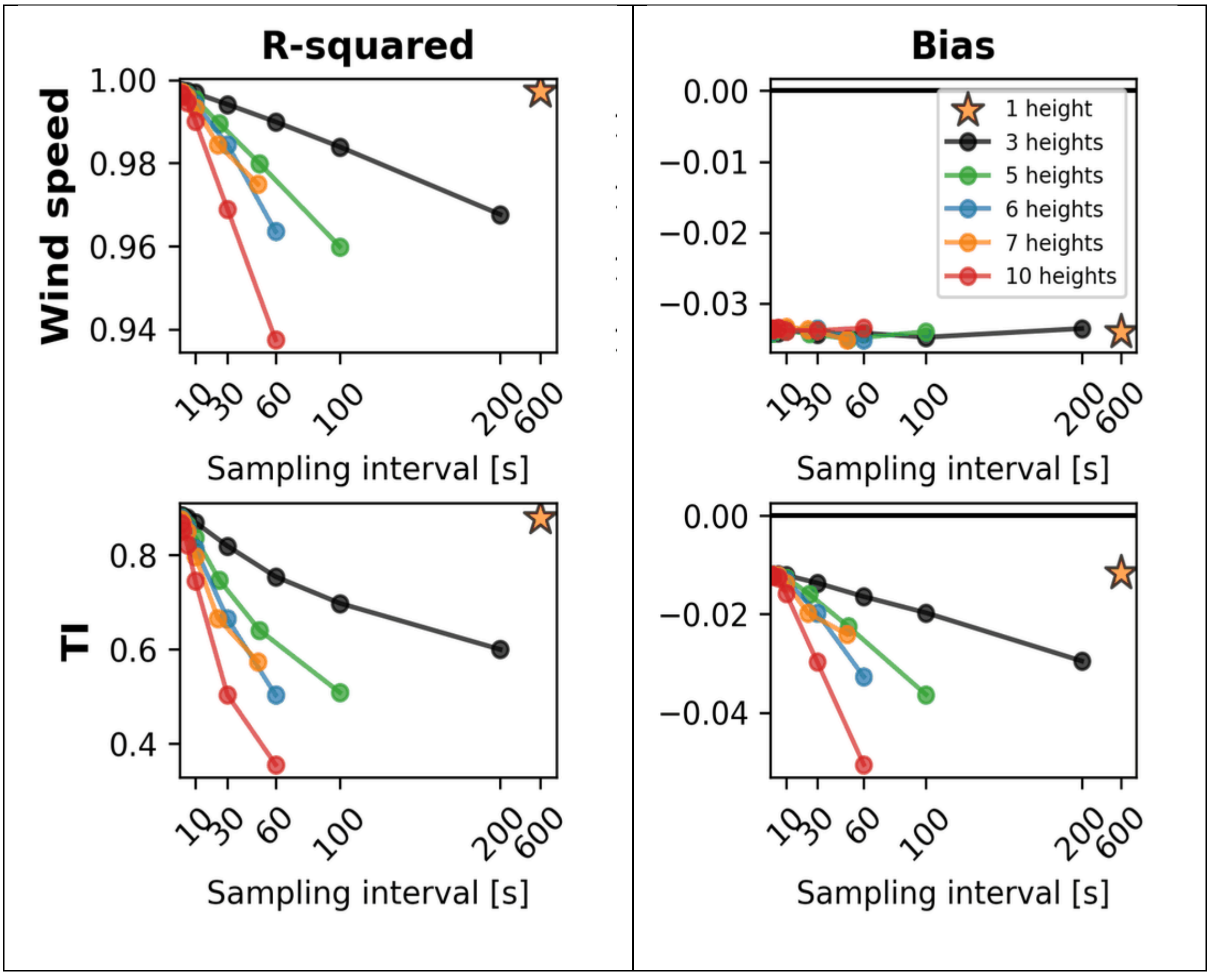

Figure 13: Impact of different Sample interval (Dwell time) on wind data quality – 10s – 600s range.

Figure 13 shows the sensitivity of measurement performance to multi-height scanning strategies. Here the best possible result is shown by the star which represents a single data point scan strategy (stare mode). Different dwell times as well as different numbers of data reconstruction points (heights) sampled, ranging from 3 (black line) to 10 (redline), show that shorter dwell times (~10 seconds) tend to give better data quality compared to longer dwell times (e.g., > 60 seconds). The results are similar to those in Watanabe et al., (2021).

Figure 14 extends this analysis to shorter dwell times of 10 s to 1s duration.

Again, we see the same trend - shorter dwell times lead to a higher correlation and lower bias for all muti-point scan scenarios, with 1 second results being very comparable to the reference mode 600s stare (star). The results indicate that short and even sampling per height is critical for minimising errors and maximising measurement performance. This result therefore should inform the approach to multi-point scan strategy development. Assuming little or no lag between the systems and that the systems can be well controlled by the scan scheduling process, for multi-point scans as short as possible dwell times produce optimal results.

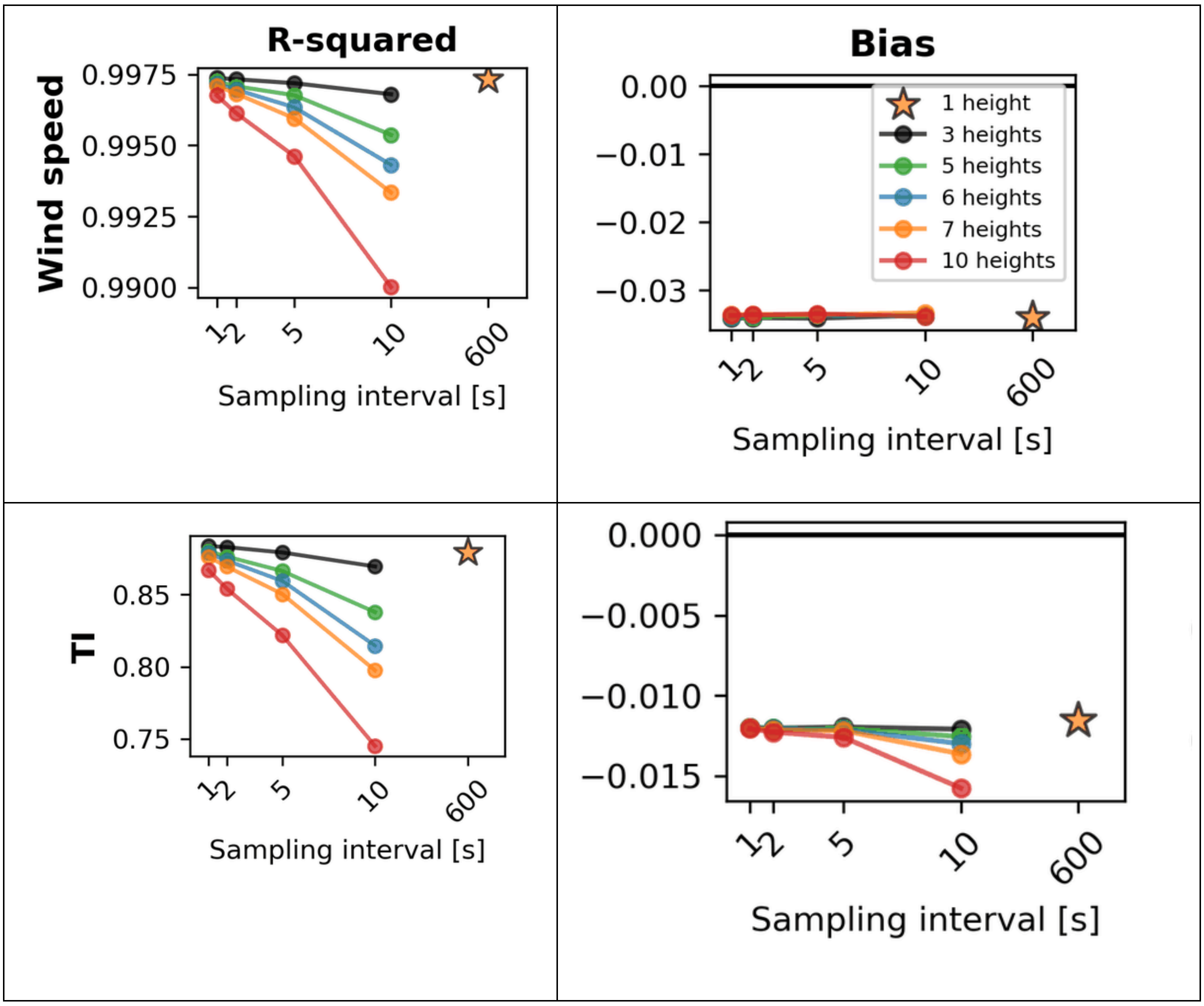

Figure 14: Extension of Watanabe study to looking at sub 10second dwell times.

In terms of the impact of time synchronisation between constituent lidars forming the DSL, Figure 15 shows the effect on data quality as an artificial lag between the measurements from the two lidars is increased from 1sto 60s.

Interestingly, temporal alignment is not a key factor for 10-min mean wind speed and direction with all results maintaining an R^2 above 0.99, but with an increasing RMSE. For TI, the performance from a time synchronisation tolerance of 1s and 2s does not change, but for longer lags the correlation quality markedly decreases with a corresponding increase in the error. We would therefore recommend no longer than a 2s time synchronisation tolerance is applied when filtering DSL measurement data.

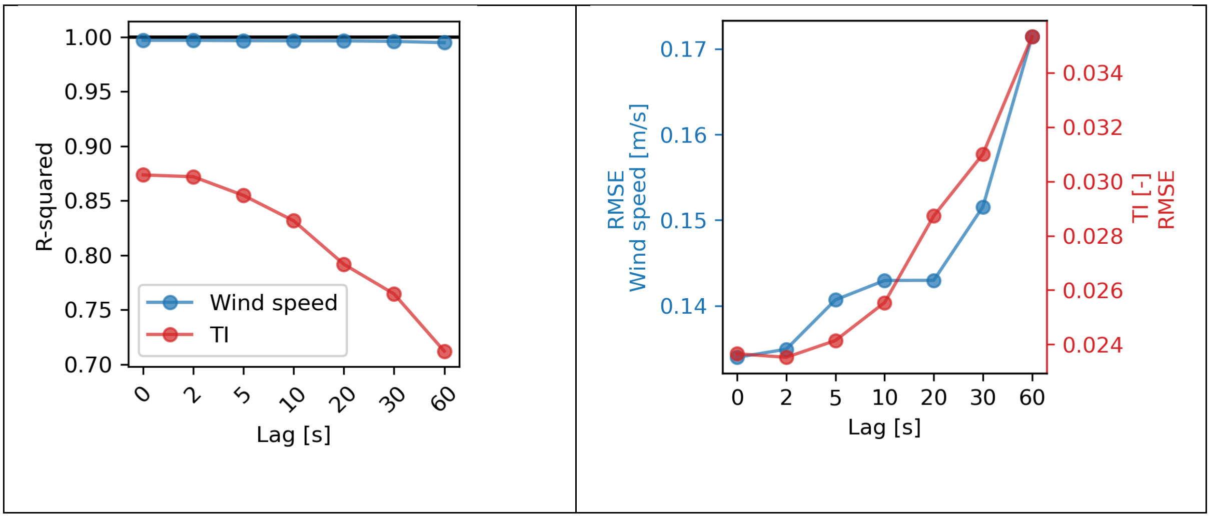

Figure 15: Time synchronization of two scanning lidars. IN creasing lag between the two datasets.

4 Discussion and Summary

The Janneby verification campaign provides quantitative evidence addressing three practical questions for dual-scanning lidar deployment in offshore wind resource assessment. The findings and recommendations are summarised as follows:

1. **<u>Overall dual-lidar measurement performance and impact of recovery rate</u>**
   Wind speed and wind direction from the dual-scanning lidar system are cup-equivalent, and high accuracy can be achieved even at relatively low sub-10-minute data availabilities (as low as ~10%). Turbulence intensity is systematically underestimated relative to cup anemometers, a limitation attributable to the lidar probe length (100 m in this configuration) rather than to the dual-lidar reconstruction method itself. Note that while recovery rate is shown to be an effective filter, applying it blankly to a measurement campaign is not recommended. Using as coarse a filter as 10% recovery rate has implications on the number of samples that are used to inform the 10-minute reconstructed wind value. It is recommended that the recovery rate lower filter be chosen with consideration of the scanning strategy and that the coarse filter recovery rate be chosen with a minimum number of samples in mind (e.g. no less than 10 samples are available within the 10-minute period – points in average)

2. **<u>Impact of long-range acquisition</u>**
   Extending measurement range primarily reduces data availability (due to declining signal-to-noise with distance) rather than degrading the fundamental accuracy of the derived wind statistics — an encouraging result for offshore campaigns that may require several kilometres of standoff distance between the lidar installation and the site of interest.

3. **<u>Measurement equivalence for multi-height scanning</u>**

Where a single dual-lidar pair is used to sample multiple heights sequentially — a common configuration for cost-effective vertical profiling — short sampling intervals (less than approximately 5 seconds per height) are important to maintain statistical equivalence with a continuous, single-height measurement, and inter-lidar time synchronisation needs to be maintained within approximately 2 seconds to preserve turbulence intensity accuracy.

Taken together, these findings support the continued development of DSL as a practical and increasingly credible substitute for physical met masts in offshore wind resource assessment, while highlighting specific engineering and operational parameters — probe length, data recovery rate, sampling interval, and dual-unit time synchronisation — that should be explicitly addressed in future recommended practices for the technology.

The authors note their thanks to the Offshore Wind Power Ltd (OWPL) consortium and the West of Orkney Windfarm development for supporting the measurement campaign that motivated this verification exercise.

5 Bibliography

CFARS. 2021. *An open source approach to evaluate the performance of remote sensing devices (RSD) Turbulence Intensity measurements & accelerate industry adoption of RSDs for turbine Site Suitability Assessment.* CFARS White Paper.

Gottschall, J., G. Wolken-Möhlmann, T. Viergutz, and B. Lange. 2014. "Results and Conclusions of a Floating-lidar Offshore Test." *Energy Procedia* 53: pp156-161.

IEC. 2022. *61400-50-2:2022, Wind Energy Generation Systems - Part 50-2: Wind measurement - Application of ground based remote sensing technology.*

IEC. 2025. *61400-50-4:2025, Wind Energy Generation Systems - Part 50-4 - Wind measurements use of floating lidar systems for wind energy measurements.*

NEDO. 2023. "Offshore measurement guidebook."

Pena, A, J. Mann, N. Angelou, and A. Jacobsen. 2022. "A Motion-Correction Method for Turbulence Estimates from Floating Lidars." https://doi.org/10.3390/rs14236065.

Shimada, S., T. Kogaki, M. Konagaya, T. Mito, R. Araki, Y. Ueda, and T. Ohsawa. 2022 . "Validation of near-shore wind measurements using a dual scanning light detection and ranging system." *Wind Energy https://doi.org/10.1002/we.2757.*

The Carbon Trust. 2018. *Carbon Trust Offshore Wind Accelerator Roadmap for the Commercial Acceptance of Floating LiDAR Technology.* The Carbon Trust.

Watanabe, K., S. Takakuwa, C. Hemmi, and T. Ishihara. 2021. "Offshore wind assessment using dual scanning lidar and missing data complement using MCP method." *Proceedings of Japan Wind Energy Symposium* 43: doi: 10.11333/jweasymppo.43_136. in Japanese

This white paper is derived from the WESC 2023 conference presentation slide deck (25/05/2023) authored by Oldbaum Services and Offshore Wind Consultants (OWC), delivered as part of IEA Wind Task 52's mini symposium on replacing met masts and accelerating offshore wind deployment.

A LLM has been used to aid with some text clarifications. LLM was not used in the results analysis or core conclusions.

This paper is written with acknowledgment to the West of Orkney project who kept an open mind to new approaches, pushing the boundaries to ensure engineering decision could be informed with the best possible data.